AGU ADVANCING EARTH AND SPACE SCIENCE

Geophysical Research Letters

RESEARCH LETTER
10.1029/2020GL088051

Changes in the Arctic Ocean Carbon Cycle With Diminishing Ice Cover

Michael DeGrandpre[1], Wiley Evans[2], Mary-Louise Timmermans[3], Richard Krishfield[4], Bill Williams[5], and Michael Steele[6]

[1]Department of Chemistry and Biochemistry, University of Montana, Missoula, MT, USA, [2]Hakai Institute, Heriot Bay, British Columbia, Canada, [3]Department of Earth and Planetary Sciences, Yale University, New Haven, CT, USA, [4]Woods Hole Oceanographic Institution, Woods Hole, MA, USA, [5]Institute of Ocean Sciences, Sidney, British Columbia, Canada, [6]Applied Physics Laboratory, University of Washington, Seattle, WA, USA

Key Points:
- The Arctic Ocean is losing ice cover at a rapid rate
- The loss of ice cover is leading to heating and uptake of atmospheric CO_2, increasing sea surface CO_2 levels
- Continued increase of sea surface CO_2 will likely reduce the uptake of atmospheric CO_2 in the future

Supporting Information:
- Supporting Information S1

Correspondence to:
M. DeGrandpre,
michael.degrandpre@umontana.edu

Citation:
DeGrandpre, M., Evans, W., Timmermans, M.-L., Krishfield, R., Williams, B., & Steele, M. (2020). Changes in the arctic ocean carbon cycle with diminishing ice cover. *Geophysical Research Letters*, *47*, e2020GL088051. https://doi.org/10.1029/2020GL088051

Received 24 MAR 2020
Accepted 12 MAY 2020
Accepted article online 24 MAY 2020

Abstract Less than three decades ago only a small fraction of the Arctic Ocean (AO) was ice free and then only for short periods. The ice cover kept sea surface pCO_2 at levels lower relative to other ocean basins that have been exposed year round to ever increasing atmospheric levels. In this study, we evaluate sea surface pCO_2 measurements collected over a 6-year period along a fixed cruise track in the Canada Basin. The measurements show that mean pCO_2 levels are significantly higher during low ice years. The pCO_2 increase is likely driven by ocean surface heating and uptake of atmospheric CO_2 with large interannual variability in the contributions of these processes. These findings suggest that increased ice-free periods will further increase sea surface pCO_2, reducing the Canada Basin's current role as a net sink of atmospheric CO_2.

Plain Language Summary The Arctic Ocean (AO) ice cover is decreasing, exposing the sea surface to exchange with the gases in the atmosphere. Consequently, anthropogenic CO_2 that has accumulated in the atmosphere can now more readily enter the AO. It is expected that this will lead to an increase in CO_2 in the AO but because of a lack of data in the region, a clear relationship has not been established. We have measured the partial pressure of CO_2 (pCO_2) in the Canada Basin of the AO during five cruises spanning 2012–2017. These data have revealed that the pCO_2 is higher during years when ice concentration is low, supporting the previous hypothesis. Using a model, we have shown that while uptake of atmospheric CO_2 has increased pCO_2, heating has also been important. These processes vary significantly from year to year, masking the likely increase in pCO_2 over time. Based on these results, we can expect that while the Canada Basin has been a sink for atmospheric CO_2, the uptake of atmospheric CO_2 will diminish in the coming years.

1. Introduction

The rapid loss of sea ice in the Arctic Ocean (AO) is well documented (Meier et al., 2014). Other changes in the AO are also becoming evident. Freshwater content is increasing due to sea ice melt and river runoff (e.g., Krishfield et al., 2014; Proshutinsky et al., 2009; Yamamoto-Kawai et al., 2009). Sea surface temperature has also increased (e.g., Perovich et al., 2011; Steele et al., 2008; Timmermans, 2015; Toole et al., 2010). This evolving physical environment is altering biological production (Arrigo & van Dijken, 2015; Bergeron & Tremblay, 2014) and food web structure (Hunt et al., 2014; Li et al., 2009; Søreide et al., 2010). The carbon cycle in the AO is intimately connected to these processes (Anderson & Macdonald, 2015), but it is not clear how carbon sources and sinks are changing in the AO and if they could affect CO_2 accumulation in the atmosphere and sea surface.

Sea surface pCO_2 is a key carbon cycle parameter because it is used to determine air-sea CO_2 fluxes for global carbon budgets and for understanding the rate of ocean acidification. Despite this, sea surface pCO_2 measurements in the AO are spatially and temporally sparse. While pCO_2 measurements date back decades (Kelley, 1970) and have continued on sporadic research cruises (Ahmed et al., 2019; Bates et al., 2006; Cai et al., 2010; Evans et al., 2015; Jutterström & Anderson, 2010; Robbins et al., 2013), measurements are mostly from AO shelf regions in the summer and fall due to limited access to more heavily ice-covered regions. Few studies have included repeat shipboard pCO_2 measurements from the AO's deep basins. The interior basins

comprise ~50% of the surface area of the AO (Bates et al., 2011) and, because of their reduced seasonal variability compared to AO coastal margins, might provide an earlier indicator of changes in pCO_2 as the ice-free sea surface is exposed to present-day atmospheric CO_2 levels.

While the AO is known to be a sink for atmospheric CO_2 (Arrigo et al., 2010; Bates et al., 2011; Islam et al., 2016, 2017; Yasunaka et al., 2016, 2018), its contribution to global air-sea CO_2 fluxes remains highly uncertain (Anderson & Macdonald, 2015). Estimated to uptake between 70 and 200 teragrams (Tg) carbon per year or 5–14% of the global uptake (Bates et al., 2011; Yasunaka et al., 2018), continued ice loss will make these estimates even more uncertain. Previous studies have found evidence that pCO_2 levels are changing in the oligotrophic AO basins and along the Chukchi shelf (Cai et al., 2010; Miller et al., 2014; Yasunaka et al., 2016, 2018), and a new analysis by Ouyang et al. (2020) more clearly shows rising levels of pCO_2 in the Canada Basin since 1994. Increased CO_2 uptake by the AO will also accelerate ocean acidification, that is, driving a commensurate decrease in pH that increases calcium carbonate solubility (Robbins et al., 2013; Yamamoto-Kawai et al., 2009). In this manuscript, a shipboard pCO_2 time series collected from 2012–2017 in the AO's Canada Basin reveals that pCO_2 increases with decreasing ice concentration. We use a temporal reference, days since ice retreat (DSR), and a mass balance model to examine to what extent ice-dependent processes such as air-sea CO_2 fluxes, surface ocean warming, and biological production drive changes in sea surface pCO_2 after ice retreats.

2. Methods

2.1. Observations

Underway sea surface pCO_2 was measured on the Beaufort Gyre Observing System/Joint Ocean Ice Study (BGOS/JOIS) cruises on the CCGS Louis S. St-Laurent during 2012–2017. No pCO_2 measurements were made in 2015. The starting dates for the five ~4 week cruises were 6 August 2012, 3 August 2013, 25 September 2014, 24 September 2016, and 8 September 2017. The pCO_2 was recorded using an infrared-gas equilibrator system (SUPER-CO_2, Sunburst Sensors, LLC) located in the ship's lab. The instrument uses an infrared analyzer (LI-COR, LI-840A) and gas phase equilibrator (Liqui-Cel membrane contactor, Model #G453) as described in Hales et al. (2004). The equilibrator was connected directly to the ship's seawater line. Calibrations were automated using CO_2 gas standards and a zero CO_2 gas sample. Temperature was measured in the equilibrator and at the seawater intake (9 m depth), assumed equal to sea surface temperature (SST), as discussed below. The infrared analyzer CO_2 mole fraction was corrected to SST and converted to pCO_2 using 100% humidity at SST and local barometric pressure (Dickson et al., 2007). Some warming, usually <0.5°C, can occur enroute to the equilibrator so it is essential to correct the pCO_2 for this temperature change. If there were greater than ~2°C differences between the equilibrator inlet temperature and SST, it was assumed seawater flow had stopped (e.g., due to ice clogging) and the pCO_2 was discarded during these periods. A flow meter was installed in 2016 to detect periods of low flow rate. The pCO_2 uncertainty is estimated to be ± 5 μatm based on the reproducibility of the standards and baseline zero. CTD stations showed that the seawater intake was sometimes within the halocline (i.e., below the mixed layer), and this was also evident from the salinity and temperature variability recorded by the ship's thermosalinograph. These conditions were found mostly on the continental shelf during 2012 and 2013 due to high Mackenzie River outflow. This analysis focuses on the Canada Basin bounded by 155–130°W and 72–82°N where CTD stations consistently found that mixed layer depths were greater than the ship intake depth.

Air temperature, wind speed, wind direction, and barometric pressure were recorded by the ship's weather system. Mixed layer depths, defined as the depth where the density difference from the surface first exceeds 0.25 kg m^{-3} (Timmermans et al., 2012), were determined using temperature and salinity from ~50 CTD casts occupied annually as part of the BGOS/JOIS cruises (Proshutinsky et al., 2019). Atmospheric pCO_2 was computed from the mole fraction of CO_2 measured at Alert, Nunavut, Canada, using data from the National Oceanic and Atmospheric Administration (NOAA) Earth System Research Laboratory (ESRL) (https://www.esrl.noaa.gov). Sea ice concentration with daily, 12 km resolution was obtained from the French Research Institute for Exploration of the Sea (IFREMER) (http://cersat.ifremer.fr/oceanography-from-space/our-domains-of-research/sea-ice) that provides data collected by the satellite-based Special Sensor Microwave Imager (SSM/I) and processed by the National Snow and Ice Data Center (https://nsidc.org).

Table 1
Mean Cruise Values Used in the Mass Balance Model Derived From Ship Measurements and Other Sources (See Section 2)

Year	Mean pCO_2 (μatm)	Sea ice concentration (%)	Wind speed (m s^{-1})	Atm. pCO_2 (μatm)	SST (°C)	Salinity	Mixed layer depth (m)
2012	365 ± 34	8 ± 22	8.1 ± 1.1	379 ± 3	2.5 ± 3.6	25.5 ± 1.4	12.1 ± 6.6
2013	327 ± 24	59 ± 38	5.0 ± 1.0	384 ± 3	−0.1 ± 1.6	26.7 ± 0.8	15.5 ± 5.5
2014	318 ± 14	78 ± 32	5.8 ± 0.7	392 ± 4	0.6 ± 2.2	27.0 ± 0.7	27.2 ± 4.3
2016	371 ± 23	21 ± 37	6.6 ± 0.3	395 ± 3	−0.3 ± 1.0	27.1 ± 0.7	26.1 ± 4.7
2017	350 ± 21	19 ± 33	7.3 ± 0.7	395 ± 2	1.1 ± 1.9	26.9 ± 1.0	26.5 ± 5.1

2.2. Data Analysis and Modeling

In this study our goals are to determine if sea surface pCO_2 levels are related to interannual variability in ice concentration and to evaluate processes that might control pCO_2 under low (or no) ice conditions. To facilitate analysis of the spatially and temporally disparate shipboard pCO_2 and other data, Canada Basin data were gridded by identifying 20 × 20 km grid areas that contain data, and those data were then averaged as described in Evans et al. (2015). Underway pCO_2 measurements collected at different times within each grid cell were averaged, and an average time of the measurements was computed. The ship might spend as much as a day within a 20 × 20 km area because of variable activities, for example, mooring deployments, so these underway data were averaged together to avoid a spatial bias. The gridding routine also computed the standard deviation of data found within each grid cell as well as the number of observations. The average number of observations for each grid cell ranged from 17–23 for each cruise. As a temporal reference relative to the beginning of the open water period, we define "days since ice retreat" or DSR, as the difference between the pCO_2 measurement date and the day of ice retreat (DOR) for each grid cell. DOR is the day when ice concentration dropped below 15% in any grid cell (Steele & Dickinson, 2016), corresponding to the approximate uncertainty in ice concentration (Ivanova et al., 2015). The gridded data were also averaged together for each cruise (i.e., each year) to allow interannual comparisons of the mean physical and biogeochemical conditions. Further, we used these yearly values as input to the mass balance model described below.

The mass balance model was used to examine how sea surface pCO_2 might change after ice retreats. Many processes contribute to sea surface pCO_2 variability in polar regions including biological production, heating and cooling, physical mixing and upwelling, ice melt and formation, and air-sea gas exchange. Sea surface warming and air-sea uptake are likely the most important factors for increasing pCO_2 in low ice areas in the Canada Basin (Cai et al., 2010; Else et al., 2013). The combined contributions of these two processes to sea surface pCO_2 variability were estimated using a dissolved inorganic carbon (DIC) mixed layer mass balance (Islam et al., 2017; Martz et al., 2009) as follows:

$$\Delta DIC = F_{\text{gasex}} \times \Delta t / (\text{MLD} \times \rho), \quad (1)$$

where ΔDIC is the change in DIC for a time step Δt (1 hr in this study), F_{gasex} is the air-sea CO_2 flux (e.g., in mmol m^{-2} day^{-1}), MLD is the mixed layer depth, and ρ is seawater density. Warming (increasing SST) is accounted for in the equilibrium calculation as described below. F_{gasex} was calculated using

$$F_{\text{gasex}} = k \times K_0 \times \Delta pCO_2 \times f, \quad (2)$$

where k is the gas transfer velocity, K_0 is the CO_2 solubility, ΔpCO_2 is the pCO_2 difference between the sea surface and atmosphere, and f is the fraction of open water (Butterworth & Miller, 2016; Prytherch et al., 2017). In this case, f is set equal to 1 because the pCO_2 was modeled only after the day of ice retreat (DOR, defined above). F_{gasex} is negative when there is a net uptake of CO_2 by the ocean from the atmosphere. We used the wind speed relationship in Wanninkhof (2014) to compute k, where ship wind speed was corrected to 10 m height. The average of second moments of wind speed (i.e., wind $speed^2$) was calculated as opposed to wind speed averages because short-term (<daily) variability in the winds is retained leading to higher gas transfer rates during periods of greater wind speed variability (Evans et al., 2015; Wanninkhof, 2014).

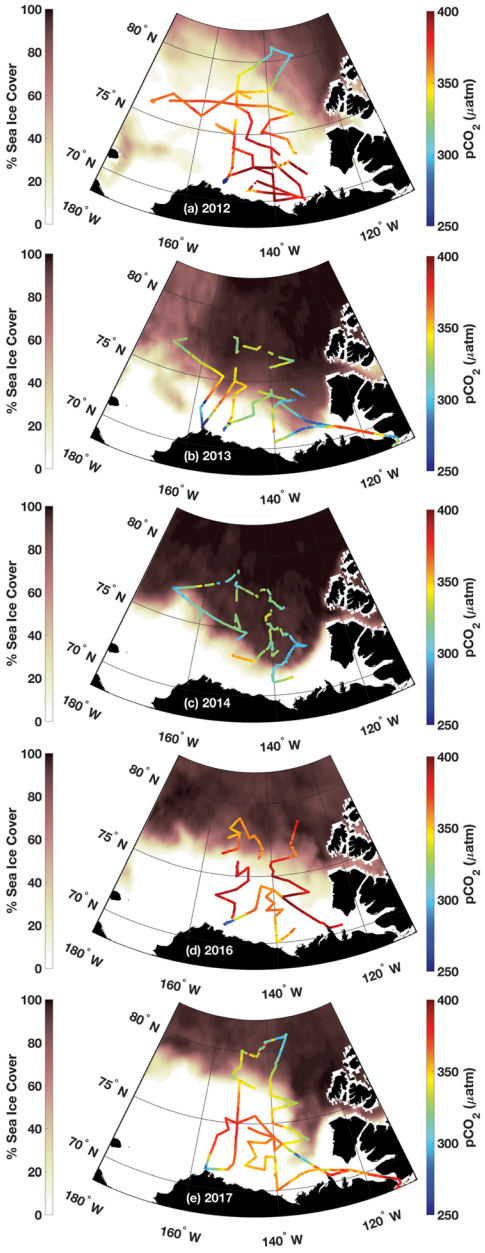

Figure 1. Sea surface partial pressure of CO_2 (pCO_2) data obtained on the Canadian icebreaker CCGS Louis S. St-Laurent from 2012–2017. The pCO_2 levels are indicated by the color along the ship cruise track (right color bar). The dark shaded coloration (left color bar) represents sea ice concentration averaged from the daily satellite data collected over the course of each cruise. Data for this analysis were taken from the area bracketed by 155–130°W, 72–82°N in the Canada Basin. The ship visited the same stations each year, but the cruise track varied to support other field studies and various other activities. The data gaps in 2013 were due to problems with the seawater intake. The starting dates for the five ~4 week cruises were 6 August 2012, 3 August 2013, 25 September 2014, 24 September 2016, and 8 September 2017, top to bottom, respectively. No pCO_2 measurements were made in 2015.

A simple modification of Equation 1 makes it possible to examine potential contributions from net community production (NCP),

$$\Delta DIC = \left(F_{\text{gasex}} + F_{\text{NCP}}\right) \times \Delta t / (\text{MLD} \times \rho), \quad (3)$$

where F_{NCP} is the net uptake of CO_2 due to biological production (e.g., in mmol m^{-2} day^{-1}). We used values from Ji et al. (2019) who measured NCP using O_2 isotope and O_2/argon methods during the same BGOS cruises, excluding 2017. In the mass balance models, DIC was incremented for each time step with ΔDIC from Equation 1 (gas exchange only) or Equation 3 (gas exchange and biological production). The pCO_2 was then recalculated using the new DIC, SST, and salinity and a constant total alkalinity (A_T) in the CO_2 equilibrium program CO2sys (Pierrot et al., 2006). The A_T was estimated using an A_T-salinity relationship derived from bottle samples during the BGOS cruises (DeGrandpre et al., 2019; Yamamoto-Kawai et al., 2005). A_T is a conservative property of seawater that does not change with temperature or air-sea CO_2 exchange (Millero, 2007). The time period of the model calculation is based on the maximum DSR for each cruise. For surface warming, SST was incremented equally for each time step from −1.5°C to the mean SST (Table 1) from DSR = 0 days until the end of the DSR period similar to Else et al. (2013). The initial under-ice condition was chosen to be the freezing point of seawater (−1.5°C) at a salinity of 27 and a seawater pCO_2 of 300 μatm all derived from extrapolation of the mean gridded data versus mean ice concentration to 100% ice concentration. All equilibrium (CO2sys) calculations used the Mehrbach et al. (1973) constants refit by Dickson and Millero (1987). Lastly, mean gridded values were used in the model calculations (Table 1 and Equations 1–3). A model that uses the evolution of ice concentration at each grid cell and includes other changing physical conditions, e.g. MLD or wind, was beyond the scope of this study.

3. Results and Discussion

The shipboard pCO_2 data collected on the Beaufort Shelf, Canada Basin, and eastern Chukchi Sea are shown in Figure 1 overlaid on % sea ice concentration. A large range of interannual variability in sea ice cover was observed during these cruises. In 2012, ice cover dropped to 3.4 million km^2, the lowest level observed since the satellite record began in 1978. The minimum ice extent rebounded in 2013 and 2014 to ~5.0 million km^2. All 5 years ranked in the top 10 lowest minima (National Snow and Ice Data Center, Arctic Sea Ice News and Analysis, http://nsidc.org/arcticseaicenews). Sea surface pCO_2 was also highly variable spatially and interannually. Open water in the Canada Basin typically had higher pCO_2 levels than pCO_2 recorded in ice-covered areas; for example, compare 2012 (low ice) and 2014 (more ice) in Figure 1.

Using the mea levels for each cruise reveals a significant correlation with ice concentration (Figure 2). Sea surface pCO_2 is higher and closer to atmospheric saturation during years of low ice concentration and exceeded atmospheric pCO_2 (Table 1) in some locations in 2012 and 2016 (Figure 1). Although sparser data sets over different regions have found evidence that sea surface pCO_2 in the AO is increasing with decreasing ice cover (Cai et al., 2010; Else et al., 2013; Jutterström &

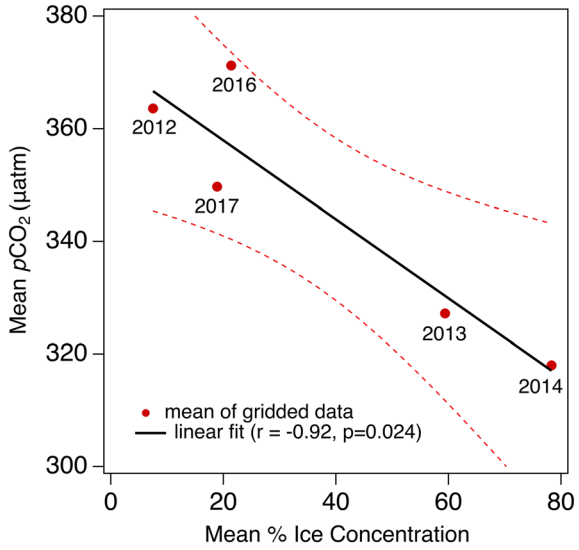

Figure 2. Canada Basin mean pCO_2 versus mean sea ice concentration for each cruise shown in Figure 1. The slope of the least squares fit is −0.70 µatm/%. Symbols are labeled with each year. Means were computed using data gridded to a 20 × 20 km area in the region spanning 155–130°W and 72–82°N (Figure S1). The 95% confidence bands are included (dashed red curves). No measurements were made in 2015.

Anderson, 2010) and a new compilation of data since 1994 shows an increase in pCO_2 in the Canada Basin (Ouyang et al., 2020), no previous studies have documented an interannual connection with ice concentration like that shown in Figure 2. The mean pCO_2 values from each cruise reveal this relationship with ice concentration by consolidating the variability—the gridded pCO_2 data for each cruise (shown in supporting information Figure S1) cover the full range shown in Figure 2 obscuring interannual differences.

The absence of sea ice exposes the surface ocean to direct solar radiation and atmospheric heating and the subsequent warming increases pCO_2. Air-sea exchange will also increase pCO_2 because, when the pCO_2 is lower than atmospheric levels, the AO will absorb CO_2 from the atmosphere (Figure 1 and Table 1). These mechanisms for increasing pCO_2 in the surface ocean suggest that pCO_2 is not only dependent upon the ice cover but also the duration of open water (Arrigo & van Dijken, 2015). Thus, the days since ice retreat (DSR) are used as a temporal reference, as defined above. We examine specific variables that might be important in driving the relationship between pCO_2 and sea ice concentration, including DSR, sea surface temperature (SST), MLD, wind speed, and NCP (Equations 1–3 and Table 1).

The gridded sea surface pCO_2 shows mostly increasing values after ice retreat with large intra and interannual variability (Figure 3a). Each year's observations appear to have a relatively consistent upward trajectory, except for 2016 and 2017 (discussed below), suggesting similar processes were at work in the open water area of the Canada Basin during each cruise. The pCO_2 observations have more scatter with increasing DSR, possibly due to different physical conditions during each cruise and each year. Some of the interannual variability may be due to differences in cruise timing, but there are significant contrasts among cruises conducted over similar periods. For example, in Figure 2, the mean pCO_2 from the August cruises (2012 and 2013) differs significantly, as do data from the late September cruises (2014 and 2017). These differences are also evident in the pCO_2 data in Figure 3a with lower values in 2013 and 2014 compared to 2012 and 2016, respectively.

The results of the mass balance model (Equation 1) assuming constant heating are shown in Figure 3a. The model encompasses the range of observed variability using the mean conditions in Table 1. Although there is

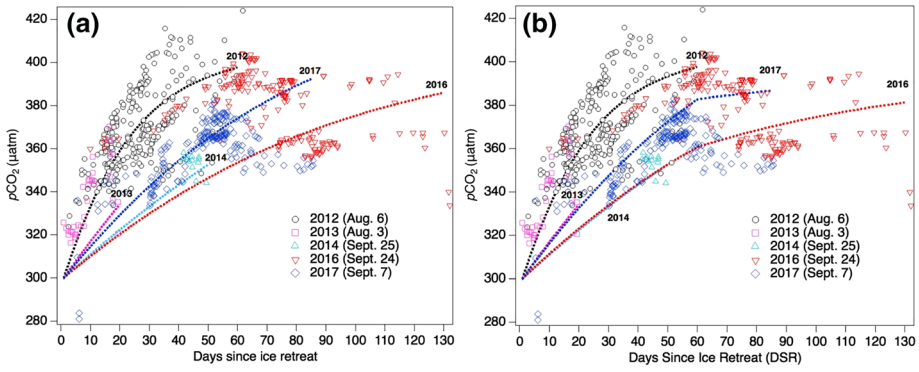

Figure 3. Gridded pCO_2 observations (symbols) versus days since ice retreat (DSR) from 2012–2017, excluding 2015. Modeled pCO_2 (dashed curves, labeled with each year and with the color matching the pCO_2 symbol data) were computed from the predicted change in pCO_2 due to air-sea exchange and increase in SST using Equation 1 and values in Table 1. Models were run to the maximum DSR recorded for each cruise period with panel (a) using a constant heating rate and panel (b) heating only until DSR = 60, then temperature is held constant. Initial pCO_2 before loss of ice was assumed to be 300 µatm (see section 2). The cruise start dates are indicated in parentheses in the legend.

disagreement between observations and model curves during some years and some parts of the records, these results suggest that heating and/or gas exchange significantly contribute to the observed increase in pCO_2 with increasing DSR and that these processes are highly variable from year to year (broken down in Figure S3). In 2012, the model predicts that heating and gas exchange increased pCO_2 by ~60 and ~30 μatm, respectively; whereas in 2016, heating and gas exchange contributions were ~15 and ~65 μatm, respectively (Figure S3). Also note that a smaller range of variability is observed and predicted for the years with shorter DSR periods (2013 and 2014) (Figures 3 and S3), where surface ocean warming and air-sea gas exchange were limited by the time of exposure to the atmosphere.

There are several other possible sources of variability and incorrect model assumptions that could contribute to differences between the model and observations. The sensitivity analysis in the Supporting Information shows that much of the variability within each cruise can be explained by varying input values over the observed ranges (Figure S2 and Table 1). There are some other notable deviations, however. For example, during 2016 and 2017, the 2 years with extended DSRs, the pCO_2 levels decreased after ~60 days (Figure 3). In these years, data were collected into October, at which point sea surface cooling is possible which would decrease the pCO_2. Because the model employs a linear warming trend, it can only predict the mean change not the time-varying rate of warming or cooling. In Figure 3b, the model was modified so that all of the heating occurred before DSR = 60, slightly steepening the pCO_2 increase but not markedly improving the prediction. We did not introduce an arbitrary period of cooling because this would essentially be fitting to the data. There is also evidence that movement of the ship into different water masses over the course of each cruise may have contributed to the variability. For example, the drop in pCO_2 after 60 days in 2017 corresponds to a period of lower salinity (not shown). Also, employing DSR as a time variable in the model assumes that no air-sea exchange or warming occurred when sea ice concentration was greater than 15% which is clearly not true (Figure S1). While we could not readily model gas exchange prior to DOR in this study, the heating contribution was small because no SST data exceeded 0.0°C from 0 to 10 days after ice retreat. An increase of −1.5°C, the approximate freezing point, to 0.0°C would increase pCO_2 by ~22 μatm. Steele and Dickinson (2016) also found that SST is typically <0°C at DOR. Ice melt and formation could change pCO_2 by diluting and concentrating DIC, respectively, and by altering the ratio of DIC and A_T in the ice or brine (Cai et al., 2010; DeGrandpre et al., 2019; Rysgaard et al., 2007, 2009). Ice melt occurs before DOR and could decrease pCO_2 levels (Cai et al., 2010). In fact, heating, gas exchange, and ice melt may have all played a role in determining the pre-DOR pCO_2 levels, contributing to the deviations between model and observations evident in Figure 3.

Lastly, we consider possible biological contributions to the observed variability. Biological drawdown of sea surface pCO_2 in the Canada Basin is predicted to be small because of the lack of nutrients in the stratified surface layer. The study by Cai et al. (2010) found no evidence of a biological DIC drawdown in the Canada Basin for waters >72°N. In a previous study in the Canada Basin, an NCP of ~4.9 mmol O_2 m^{-2} day^{-1} offset a ~15 μatm pCO_2 increase expected from atmospheric CO_2 uptake in low ice conditions (Islam et al., 2017). The Ji et al. (2019) NCP values, which ranged from 1.3 to 2.9 mmol O_2 m^{-2} day^{-1} from 2011–2016, confirm the very low productivity for the Canada Basin (Bates et al., 2005). For comparison, in the same paper, NCP in the eastern Chukchi Sea was estimated to range from 30 to 240 mmol m^{-2} day^{-1}. The Canada Basin rates have a relatively small effect on the modeled pCO_2 levels, estimated using Equation 3 (Figure S2). In 2012, the pCO_2 would be reduced by 8–25 μatm by the end of the DSR period (60 days) over the range of NCP reported in Ji et al. (2019). These estimates assume the rate of NCP was constant over the DSR period. The O_2/argon method integrates NCP over the residence time of O_2 in the mixed layer (10–30 days) (Kaiser et al., 2005) and the rates in Ji et al. (2019) varied by only 15–21% during the cruises. This range of variability would not significantly alter the modeled pCO_2 trajectory (Figure S2 and Table S1).

4. Conclusions

This study reveals that loss of sea ice leads to large interannual changes in sea surface pCO_2 levels in the Canada Basin. Using the DSR as a temporal reference facilitated implementation of a time-dependent mass balance model to explore the underlying mechanisms that might control sea surface pCO_2 in open water conditions. Results from the model suggest that warming and air-sea uptake drive the pCO_2 toward

atmospheric equilibrium to a varying extent (Figures 3 and S3). NCP is persistently low and can only account for a small portion of the observed interannual variability (Figure S2 and Table S1). These results suggest that neither of two previously proposed scenarios, that is, that increased SST will largely negate uptake of atmospheric CO_2 (Else et al., 2013) or that air-sea gas exchange, will consistently dominate the increase in pCO_2 (Bates et al., 2006; Cai et al., 2010) (Figure S2). An important implication, as discussed by others (Cai et al., 2010), is that increased SSTs can reduce the uptake of atmospheric CO_2 by increasing the rate at which pCO_2 rises toward atmospheric equilibrium, decreasing the air-sea CO_2 gradient. The model simulation suggests that warming reduced the possible air-sea CO_2 flux by 55% in 2012, the year with the most warming (Figure S3). As Arctic warming and open water periods increase, it is possible that, as observed in 2012, the lowest ice concentration year on record, pCO_2 will more frequently exceed atmospheric saturation. Over the period covered in this study any accumulation of CO_2 is hidden by the interannual variability of ice cover, but the study by Ouyang et al. (2020) over a 23 year period clearly reveals this expected CO_2 increase in the Canada Basin. Even with the insights provided in these new data sets, the future response of the AO carbon cycle to decreased seasonal ice cover remains highly uncertain and can only be understood by continued observations and modeling.

Data Availability Statement

The data are available through the U.S. National Science Foundation (NSF) Arctic Data Center (https://arcticdata.io) (doi:10.18739/A2R785P3X).

Acknowledgments

Cory Beatty (University of Montana) operated the underway pCO_2 system. Fakhrul Islam and Brittany Peterson (University of Montana) helped with data analysis. Sarah Zimmerman (Institute of Ocean Sciences) facilitated installation of the pCO_2 system and oversaw the seawater line measurements. The underway pCO_2 instrument (SUPER-CO_2) and technical support were provided by Sunburst Sensors. We thank Andrey Proshutinsky (WHOI) for his leadership as co-PI of the BGOS program. Additional vital logistical support was provided by WHOI personnel. The reviewers' comments significantly improved the manuscript. This research was made possible by grants from the NSF Arctic Observing Network program (ARC-1107346, PLR-1302884, PLR-1504410, and OPP-1723308). In addition, M. S. was supported by ONR (Grant 00014-17-1-2545), NASA (Grant NNX16AK43G), and NSF (Grants PLR-1503298 and OPP-1751363).

References

Ahmed, M., Else, B. G. T., Burgers, T. M., & Papakyriakou, T. (2019). Variability of surface water pCO_2 in the Canadian Arctic Archipelago from 2010 to 2016. *Journal of Geophysical Research: Oceans*, *124*, 1876–1896. https://doi.org/10.1029/2018JC014639

Anderson, L. G., & Macdonald, R. W. (2015). Observing the Arctic Ocean carbon cycle in a changing environment. *Polar Research*, *34*(1), 26,891. https://doi.org/10.3402/polar.v34.26891

Arrigo, K. R., Pabi, S., van Dijken, G. L., & Maslowski, W. (2010). Air-sea flux of CO_2 in the Arctic Ocean, 1998–2003. *Journal of Geophysical Research*, *115*, G04024. https://doi.org/10.1029/2009JG001224

Arrigo, K. R., & van Dijken, G. L. (2015). Continued increases in Arctic Ocean primary production. *Progress in Oceanography*, *136*, 60–70. https://doi.org/10.1016/j.pocean.2015.05.002

Bates, N. R., Best, M. H. P., & Hansell, D. A. (2005). Spatio-temporal distribution of dissolved inorganic carbon and net community production in the Chukchi and Beaufort seas. *Deep Sea Research Part II: Topical Studies in Oceanography*, *52*(24-26), 3303–3323. https://doi.org/10.1016/j.dsr2.2005.10.005

Bates, N. R., Cai, W.-J., & Mathis, J. T. (2011). The ocean carbon cycle in the western Arctic Ocean: Distributions and air-sea fluxes of carbon dioxide. *Oceanography*, *24*(3), 186–201. https://doi.org/10.5670/oceanog.2011.71

Bates, N. R., Moran, S. B., Hansell, D. A., & Mathis, J. T. (2006). An increasing CO_2 sink in the Arctic Ocean due to sea-ice loss. *Geophysical Research Letters*, *33*, L23609. https://doi.org/10.1029/2006GL027028

Bergeron, M., & Tremblay, J.-É. (2014). Shifts in biological productivity inferred from nutrient drawdown in the southern Beaufort Sea (2003–2011) and northern Baffin Bay (1997–2011), Canadian Arctic. *Geophysical Research Letters*, *41*, 3979–3987. https://doi.org/10.1002/2014GL059649

Butterworth, B. J., & Miller, S. D. (2016). Air-sea exchange of carbon dioxide in the Southern Ocean and Antarctic marginal ice zone. *Geophysical Research Letters*, *43*, 7223–7230. https://doi.org/10.1002/2016GL069581

Cai, W., Grebmeier, J. M., Hu, X., Lee, S. H., Murata, A., Sullivan, K., et al. (2010). Decrease in the CO_2 uptake capacity in an ice-free Arctic Ocean basin. *Science*, *329*(5991), 556–559. https://doi.org/10.1126/science.1189338

DeGrandpre, M. D., Lai, C.-Z., Timmermans, M.-L., Krishfield, R. A., Proshutinsky, A., & Torres, D. (2019). Inorganic carbon and pCO_2 variability during ice formation in the Beaufort Gyre of the Canada Basin. *Journal of Geophysical Research: Oceans*, *124*, 4017–4028. https://doi.org/10.1029/2019JC015109

Dickson, A., & Millero, F. (1987). A comparison of the equilibrium constants for the dissociation of carbonic acid in seawater media. *Deep-Sea Research Part A*, *34*(10), 1733–1743. https://doi.org/10.1016/0198-0149(87)90021-5

Dickson, A. G., Sabine, C. L., & Christian, J. R. (Eds) (2007). *Guide to best practices for ocean CO_2 measurements* (Vol. 3, p. 191). North Pac. Mar. Sci. Organ., Sidney, B. C., Canada: PICES Special Publication. https://doi.org/10.1039/9781847550835

Else, G. T., Galley, R. J., Lansard, B., Barber, D. G., Brown, K., Miller, L. A., et al. (2013). Further observations of a decreasing atmospheric CO_2 uptake capacity in the Canada Basin (Arctic Ocean) due to sea ice loss. *Geophysical Research Letters*, *40*, 1132–1137. https://doi.org/10.1002/grl.50268

Evans, W., Mathis, J. T., Cross, J. N., Bates, N. R., Frey, K. E., Else, B. G. T., et al. (2015). Sea-air CO_2 exchange in the western Arctic coastal ocean. *Global Biogeochemical Cycles*, *29*, 1190–1209. https://doi.org/10.1002/2015GB005153

Hales, B., Chipman, D. W., & Takahashi, T. (2004). High frequency measurement of partial pressure and total concentration of carbon dioxide in seawater using microporous hydrophobic membrane contactors. *Limnology and Oceanography: Methods*, *2*, 356–364.

Hunt, B. P. V., Nelson, R. J., Williams, B., McLaughlin, F. A., Young, K., Brown, K. A., et al. (2014). Zooplankton community structure and dynamics in the Arctic Canada Basin during a period of intense environmental change (2004–2009). *Journal of Geophysical Research: Oceans*, *119*, 2518–2538. https://doi.org/10.1002/2013JC009156

Islam, F., DeGrandpre, M., Beatty, C., Krishfield, R., & Toole, J. (2016). Gas exchange of CO_2 and O_2 in partially ice-covered regions of the Arctic Ocean investigated using in situ sensors. *IOP. Conf. Series: Earth and Environmental Science*, *35*, 012018. https://doi.org/10.1088/1755-1315/35/1/012018

Islam, F., DeGrandpre, M., Beatty, C., Timmermans, M.-L., Krishfield, R., Toole, J., & Laney, S. (2017). Sea surface pCO_2 and O_2 dynamics in the partially ice-covered Arctic Ocean. *Journal of Geophysical Research: Oceans*, *122*, 1425–1438. https://doi.org/10.1002/2016JC012162

Ivanova, N., Pedersen, L. T., Tonboe, R. T., Kern, S., Heygster, G., Lavergne, T., et al. (2015). Inter-comparison and evaluation of sea ice algorithms: Towards further identification of challenges and optimal approach using passive microwave observations. *The Cryosphere*, *9*(5), 1797–1817. https://doi.org/10.5194/tc-9-1797-2015

Ji, B. Y., Sandwith, Z. O., Williams, W. J., Diaconescu, O., Ji, R., Li, Y., et al. (2019). Variations in rates of biological production in the Beaufort Gyre as the Arctic changes: Rates from 2011 to 2016. *Journal of Geophysical Research: Oceans*, *124*, 3628–3644. https://doi.org/10.1029/2018JC014805

Jutterström, S., & Anderson, L. G. (2010). Uptake of CO_2 by the Arctic Ocean in a changing climate. *Marine Chemistry*, *122*(1-4), 96–104. https://doi.org/10.1016/j.marchem.2010.07.002

Kaiser, J., Reuer, M. K., Barnett, B., & Bender, M. L. (2005). Marine productivity estimates from continuous O_2/Ar ratio measurements by membrane inlet mass spectrometry. *Geophysical Research Letters*, *32*, L19605. https://doi.org/10.1029/2005GL023459

Kelley, J. J. Jr. (1970). Carbon dioxide in the surface waters of the North Atlantic and the Barents and Kara Sea. *Limnology and Oceanography*, *15*(1), 80–87. https://doi.org/10.4319/lo.1970.15.1.0080

Krishfield, R. A., Proshutinsky, A., Tateyama, K., Williams, W. J., Carmack, E. C., McLaughlin, F. A., & Timmermans, M.-L. (2014). Deterioration of perennial sea ice in the Beaufort Gyre from 2003 to 2012 and its impact on the oceanic freshwater cycle. *Journal of Geophysical Research*, *119*, 1271–1305. https://doi.org/10.1002/2013JC008999

Li, W. K., McLaughlin, F. A., Lovejoy, C., & Carmack, E. C. (2009). Smallest algae thrive as the Arctic Ocean freshens. *Science*, *326*(5952), 539–539. https://doi.org/10.1126/science.1179798

Martz, T. M., DeGrandpre, M. D., Strutton, P. G., McGillis, W. R., & Drennan, W. (2009). Sea surface pCO_2 and carbon export during the Labrador Sea spring-summer bloom: an in situ mass balance approach. *Journal of Geophysical Research*, *114*, C09008. https://doi.org/10.1029/2008JC005060

Mehrbach, C., Culberson, C. H., Hawley, J. E., & Pytkowicz, R. M. (1973). Measurement of the apparent dissociation constants of carbonic acid in seawater at atmospheric pressure. *Limnology and Oceanography*, *18*(6), 897–907. https://doi.org/10.4319/lo.1973.18.6.0897

Meier, W. N., Hovelsrud, G. K., van Oort, B. E. H., Key, J. R., Kovacs, K. M., Michel, C., et al. (2014). Arctic Sea ice in transformation: A review of recent observed changes and impacts on biology and human activity. *Reviews of Geophysics*, *52*, 185–217. https://doi.org/10.1002/2013RG000431

Miller, L. A., Macdonald, R. W., Mucci, A., Yamamoto-Kawai, M., Giesbrecht, K. E., McLaughlin, F., & Williams, W. J. (2014). Changes in the marine carbonate system of the western Arctic: Patterns in a rescued data set. *Polar Research*, *33*(1), 20,577. https://doi.org/10.3402/polar.v33.20577

Millero, F. J. (2007). The marine inorganic carbon cycle. *Chemical Reviews*, *107*(2), 308–341. https://doi.org/10.1021/cr0503557

Ouyang, Z., Qi, D., Chen, L., Zhong, W., Takahashi, T., DeGrandpre, M. D., et al. (2020). Sea-ice loss amplifies summer-time decadal CO_2 increase in the western Arctic Ocean. *Nature Climate Change*. Accepted.

Perovich, D., Jones, K., Light, B., Eicken, H., Markus, T., Stroeve, J., & Lindsay, R. (2011). Solar partitioning in a changing Arctic Sea-ice cover. *Annals of Glaciology*, *52*(57), 192–196. https://doi.org/10.3189/172756411795931543

Pierrot, D., Lewis, E., & Wallace, D. W. R. (2006). MS Excel program developed for CO_2 system calculations. ORLN/CDIAC-105, Carbon Dioxide Information Analysis Center, Oak Ridge National Laboratory, U.S. Department of Energy, Oak Ridge, Tennessee.

Proshutinsky, A., Krishfield, R., & Timmermans, M.-L. (2019). Preface to special issue forum for Arctic Ocean modeling and observational synthesis (FAMOS) 2: Beaufort gyre phenomenon. *Journal of Geophysical Research: Oceans*, *125*. https://doi.org/10.1029/2019JC015400

Proshutinsky, A., Krishfield, R., Timmermans, M.-L., Toole, J., Carmack, E., McLaughlin, F., et al. (2009). Beaufort Gyre freshwater reservoir: State and variability from observations. *Journal of Geophysical Research*, *114*, C00A10. https://doi.org/10.1029/2008JC005104

Prytherch, J., Brooks, I. M., Crill, P. M., Thornton, B. F., Salisbury, D. J., Tjernström, M., et al. (2017). Direct determination of the air-sea CO_2 gas transfer velocity in Arctic Sea ice regions. *Geophysical Research Letters*, *44*, 3770–3778. https://doi.org/10.1002/2017GL073593

Robbins, L. L., Wynn, J. G., Lisle, J. T., Yates, K. K., Knorr, P. O., Byrne, R. H., et al. (2013). Baseline monitoring of the western Arctic Ocean estimates 20% of Canadian Basin surface waters are undersaturated with respect to aragonite. *PLoS ONE*, *8*(9), e73796. https://doi.org/10.1371/journal.pone.0073796

Rysgaard, S., Bendtsen, J., Pedersen, L. T., Ramløv, H., & Glud, R. N. (2009). Increased CO_2 uptake due to sea ice growth and decay in the Nordic seas. *Journal of Geophysical Research*, *114*, C09011. https://doi.org/10.1029/2008JC005088

Rysgaard, S., Glud, R. N., Sejr, M. K., Bendtsen, J., & Christensen, P. B. (2007). Inorganic carbon transport during sea ice growth and decay: A carbon pump in polar seas. *Journal of Geophysical Research*, *112*, C03016. https://doi.org/10.1029/2006JC003572

Søreide, J. E., Leu, E. V. A., Berge, J., Graeve, M., & Falk-Petersen, S. (2010). Timing of blooms, algal food quality and *Calanus glacialis* reproduction and growth in a changing Arctic. *Global Change Biology*, *16*, 3154–3163.

Steele, M., & Dickinson, S. (2016). The phenology of Arctic Ocean surface warming. *Journal of Geophysical Research: Oceans*, *121*, 6847–6861. https://doi.org/10.1002/2016JC012089

Steele, M., Ermold, W., & Zhang, J. (2008). Arctic Ocean surface warming trends over the past 100 years. *Geophysical Research Letters*, *35*, L02614. https://doi.org/10.1029/2007GL031651

Timmermans, M.-L. (2015). The impact of stored solar heat on Arctic Sea-ice growth. *Geophysical Research Letters*, *42*, 6399–6406. https://doi.org/10.1002/2015GL064541

Timmermans, M.-L., Cole, S., & Toole, J. (2012). Horizontal density structure and restratification of the Arctic Ocean surface layer. *Journal of Physical Oceanography*, *42*, 659–668. https://doi.org/10.1175/JPO-D-11-0125.1

Toole, J. M., Timmermans, M.-L., Perovich, D. K., Krishfield, R. A., Proshutinsky, A., & Richter-Menge, J. A. (2010). Influences of the ocean surface mixed layer and thermohaline stratification on Arctic Sea ice in the Central Canada Basin. *Journal of Geophysical Research*, *115*, C10018. https://doi.org/10.1029/2009JC005660

Wanninkhof, R. (2014). Relationship between wind speed and gas exchange over the ocean revisited. *Limnology and Oceanography: Method*, *12*(6), 351–362. https://doi.org/10.4319/lom.2014.12.351

Yamamoto-Kawai, M., McLaughlin, F. A., Carmack, E. C., Nishino, S., & Shimada, K. (2009). Aragonite undersaturation in the Arctic Ocean: Effects of ocean acidification and sea ice melt. *Science*, *326*(5956), 1098–1100. https://doi.org/10.1126/science.1174190

Yamamoto-Kawai, M., Tanaka, N., & Pivovarov, S. (2005). Freshwater and brine behaviors in the Arctic Ocean deduced from historical data of $\delta^{18}O$ and alkalinity (1929–2002 A.D.). *Journal of Geophysical Research*, *110*, C10003. https://doi.org/10.1029/2004JC002793

Yasunaka, S., Murata, A., Watanabe, E., Chierici, M., Fransson, A., van Heuven, S., et al. (2016). Mapping of the air–sea CO_2 flux in the Arctic Ocean and its adjacent seas: Basin-wide distribution and seasonal to interannual variability. *Polar Science*, *10*(3), 323–334. https://doi.org/10.1016/j.polar.2016.03.006

Yasunaka, S., Siswanto, E., Olsen, A., Hoppema, M., Watanabe, E., Fransson, A., et al. (2018). Arctic Ocean CO_2 uptake: An improved multiyear estimate of the air–sea CO_2 flux incorporating chlorophyll *a* concentrations. *Biogeosciences*, *15*, 1643–1661. https://doi.org/10.5194/bg-15-1643-2018